NeuroImage: Clinical 50 (2026) 104012

Contents lists available at ScienceDirect

NeuroImage: Clinical

journal homepage: www.elsevier.com/locate/ynicl

Structural-functional multilayer brain network properties and outcome of combined repetitive transcranial magnetic stimulation and psychotherapy for obsessive–compulsive disorder

Sophie M.D.D. Fitzsimmons [a,b,*], Coen Coomans [a,b], Lucas Breedt [b], Neeltje M. Batelaan [a,b,d,e], Ysbrand D. van der Werf [b,c], Odile A. van den Heuvel [a,b,c], Linda Douw [b,1], Chris Vriend [a,b,c,1]

[a] Amsterdam UMC, Vrije Universiteit Amsterdam, Department of Psychiatry, de Boelelaan 1117, Amsterdam, the Netherlands
[b] Amsterdam UMC, Vrije Universiteit Amsterdam, Department of Anatomy & Neurosciences, de Boelelaan 1117, Amsterdam, the Netherlands
[c] Amsterdam Neuroscience, Compulsivity, Impulsivity & Attention program, Amsterdam, the Netherlands
[d] Amsterdam Public Health, Amsterdam, the Netherlands
[e] GGZ inGeest, Amsterdam, the Netherlands

ARTICLE INFO

Keywords:
Repetitive transcranial magnetic stimulation
Obsessive–compulsive disorder
Graph analysis
Multilayer networks
Functional MRI
Diffusion MRI

ABSTRACT

Background: Repetitive transcranial magnetic stimulation (rTMS) is a promising treatment for obsessive–compulsive disorder (OCD), but response rates are variable. Pre-treatment characteristics of the stimulated region can influence rTMS outcome.
Objective/hypothesis: We investigated the relationship between network features of the rTMS stimulation location and treatment outcome in a randomised trial of rTMS combined with exposure and response prevention psychotherapy (ERP) for OCD, using graph analysis of single-layer functional and structural brain networks, and of structural–functional multilayer networks.
Methods: We analysed data from 58 treatment-refractory adult OCD patients. Participants received either: high frequency (HF) rTMS to the left dorsolateral prefrontal cortex (DLPFC) (n = 19); HF rTMS to the left pre-supplementary motor area (preSMA) (n = 21); or control rTMS to the vertex (n = 18), all combined with ERP. We used pre-treatment resting state functional MRI (rs-fMRI) and diffusion MRI (dMRI) scans to construct single-layer and structural–functional multilayer networks for each participant. We computed various centrality measures of the stimulated location and subnetwork, and examined their relationship with treatment outcome.
Results: We found no associations between functional/structural single-layer network characteristics and treatment outcome. However, higher average multilayer betweenness centrality of the stimulated subnetwork in the DLPFC rTMS group (but not in the preSMA/vertex groups) was associated with symptom reduction ($p = 0.013$).
Conclusions: Participants with greater integration of the stimulated subnetwork with the rest of the structural–functional network showed greater improvement following DLPFC rTMS-ERP. Our exploratory results give a preliminary indication of the importance of the interplay between structural and functional networks for rTMS outcome.

1. Introduction

Repetitive transcranial magnetic stimulation (rTMS) is an increasingly prevalent non-invasive brain stimulation treatment technique in psychiatry, primarily used for depression, but also showing promise for several other disorders, including obsessive–compulsive

Abbreviations: rTMS, repetitive transcranial magnetic stimulation; OCD, obsessive–compulsive disorder; FC, functional connectivity; DLPFC, dorsolateral prefrontal cortex; dMRI, diffusion MRI; rsfMRI, resting state functional MRI; tbfMRI, task based functional MRI; ERP, exposure and response prevention; YBOCS, Yale Brown Obsessive Compulsive Scale; SRI, serotonin reuptake inhibitor; preSMA, pre-supplementary motor area; NS, node strength; BC, betweenness centrality; PC, participation coefficient; EC, eigenvector centrality; DC, degree centrality.

* Corresponding author at: Amsterdam UMC, Vrije Universiteit Amsterdam, Department of Psychiatry, de Boelelaan 1117, Amsterdam, the Netherlands.
E-mail address: s.fitzsimmons@amsterdamumc.nl (S.M.D.D. Fitzsimmons).
[1] joint last authors.

https://doi.org/10.1016/j.nicl.2026.104012
Received 5 December 2025; Received in revised form 22 May 2026; Accepted 25 May 2026
Available online 26 May 2026

disorder (OCD) (Hyde et al., 2022; Kan et al., 2023; Lefaucheur et al., 2020). RTMS works by delivering a train of magnetic pulses to a specific brain region, inducing neuroplasticity: changes in brain structure and function at both the stimulation location and distant connected regions that are related to clinical improvements (Siebner et al., 2022; Fitzsimmons et al., 2024). Response to rTMS is, however, variable, partly due to inter-individual variation in the neurobiological properties of the targeted brain area and (sub)network. There is substantial evidence from studies of rTMS treatment for depression that the functional connectivity (FC) (or correlation between activity fluctuations) of the stimulation location with other connected brain regions has an influence on rTMS response: for example, FC of the dorsolateral prefrontal cortex (DLPFC) with the subgenual anterior cingulate cortex (Fox et al., 2012; Cash et al., 2019; Cash et al., 2021; Weigand et al., 2018) is associated with rTMS treatment outcome. There is also evidence to suggest that structural, white-matter connectivity is a mediator of rTMS effect: diffusion MRI (dMRI) measures such as fractional anisotropy or streamline count close to the stimulated area have been found to be related to rTMS outcome in depression (Klooster et al., 2020; Barredo et al., 2019; Ning et al., 2022).

Connectivity is only one brain feature related to rTMS response: the spatial organisation or topology of the brain network may also be relevant. The topology of the brain network can be described using graph/network analysis, where nodes of the network are brain areas, defined by an atlas, and their connections are defined by the correlation in activity between nodes (for functional MRI (fMRI)-derived connectomes) or by the number of streamlines (for dMRI-derived structural connectomes) (Bullmore and Sporns, 2009). Graph metrics describe the organisation of the network or the role of a specific node in the network: for example, centrality measures indicate the extent to which a node can influence or be influenced by other nodes by describing various aspects of its connectivity (Fornito, 2016). Studies of single-session rTMS in both controls (Fitzsimmons et al., 2020) and OCD patients (Douw et al., 2020) using centrality graph measures extracted from fMRI networks have shown that greater baseline local connectivity (i.e. connectivity to neighbouring nodes) and less integration (i.e. connectivity throughout the entire network) of the stimulation site and stimulated network is associated with greater rTMS effects. This approach is, however, reductionistic: The functional brain network is dependent on and constrained by the structural network (Honey et al., 2007; Deco et al., 2011; Honey et al., 2009): examining the combined contributions of functional and structural connectivity may have greater explanatory value than either type of connectivity alone (Breedt et al., 2023; de Kwaasteniet et al., 2013).

One method of examining the combination of brain structure and function is by constructing multilayer networks (Breedt et al., 2023; De Domenico, 2017; Battiston et al., 2017), which consist of multiple linked networks with the same nodes but different edge definitions (for example, a two-layer network with links defined by rsfMRI and by dMRI). It is thought that multilayer brain networks capture the interplay between different network layers that analysing modalities separately may miss (De Domenico, 2017; Simas et al., 2015), and allow the integration of multiple sources of information about network organisation, providing a better representation of the multimodal nature of brain networks. A recent study by Breedt et al (Breedt et al., 2023) showed that while centrality of single layer rsfMRI-, dMRI- or resting-state MEG-derived networks did not predict executive function in controls, centrality of the multilayer network did. Other studies have highlighted the clinical relevance of multilayer networks, showing that multilayer network features can discriminate between healthy controls and Alzheimer's disease (Guillon et al., 2017) and schizophrenia (De Domenico et al., 2016), and track longitudinal changes in executive function in glioma patients (van Lingen et al., 2023).

In this exploratory study, we used neuroimaging data from a recent clinical trial of combined rTMS and exposure and response prevention psychotherapy (ERP) for OCD (Fitzsimmons et al., 2023) to examine the association between treatment outcome and rsfMRI- and dMRI-derived single- and multilayer network features of the stimulated network and stimulation location.

We investigated:

1. whether baseline graph features of functional and structural single-layer networks were associated with treatment outcome.
2. whether baseline graph features of a structural–functional multilayer network were associated with treatment outcome.

For single-layer functional networks, we hypothesised that higher local connectivity and lower global connectivity would be associated with greater response to rTMS. We expected to see the same direction of effect for structural as for functional graph features, because structural connectivity is generally correlated with FC (Honey et al., 2009) (though this can vary across the cortex (Vázquez-Rodríguez et al., 2019), and studies examining other dMRI connectivity features (Klooster et al., 2020; Barredo et al., 2019; Ning et al., 2022) also suggest that greater local connectivity may predict greater rTMS effects. There is no literature on the relationship between rTMS effects and multilayer network organisation. Given that structural–functional multilayer networks summarise the combined contribution of structural and functional graph features, we hypothesised the same directions of effect as for single-layer graph measures.

2. Material and methods

2.1. Participants

This study uses data from the TIPICCO trial (TMS-induced plasticity improving cognitive control in OCD, registered at NCT03667807). Full methods are reported elsewhere (Fitzsimmons et al., 2023). Sixty-four adults with OCD started the treatment. Eligibility criteria were: meeting DSM-5 criteria for OCD as determined by the Structured Clinical Interview for DSM-5 (First et al., 2016), moderate/severe OCD symptoms (Yale-Brown Obsessive-Compulsive Scale (Goodman et al., 1989) (YBOCS) score of $\geq$ 16), age 18–65 years, previous treatment with $\geq$ 8 sessions of ERP or cognitive-behavioural therapy for OCD, and $\geq$ 12 weeks of previous serotonin reuptake inhibitor (SRI) treatment for OCD or medication naïve due to a strong preference for non-pharmacological treatment. Exclusion criteria were: Tourette's syndrome, schizophrenia, bipolar disorder, active suicidal ideation, MRI/rTMS exclusion criteria, and previous experience with rTMS. Participants were allowed to continue current SRI medication at the same dose. The study was approved by the ethics committee of the VU Medical Center (VUmc), Amsterdam, The Netherlands, and was conducted as a collaboration between the VUmc and the mental health care institute GGZ inGeest, Amsterdam. All participants provided written informed consent in accordance with the declaration of Helsinki.

2.2. Study design

This was a three-arm parallel randomised controlled trial, conducted between May 2019 and October 2022. Participants were randomised to one of three types of rTMS (10 Hz, targeting either L DLPFC or L pre-supplementary motor area [preSMA] at 110% motor threshold, or vertex at 60% motor threshold as a control condition), all immediately followed by ERP. This was delivered twice a week, for 8 weeks (20 treatment sessions in total, of which 16 were rTMS-ERP sessions and 4 ERP only). Individualised coordinates for neuronavigated targeting of rTMS for the DLPFC and preSMA groups were determined using task-based fMRI acquired at baseline (T0) (during the Tower of London task for the DLPFC, and the Stop-signal task for the preSMA) (see Supplement and (Fitzsimmons et al., 2023) for full details of rTMS and ERP treatments, and rTMS target determination). OCD symptom severity was assessed using the YBOCS at T0, after rTMS-ERP session 8 (T1), after

rTMS-ERP session 16 (T2), and 12 weeks following the end of treatment (T3); only measurements from T0 and T2 are used in this study. Participants also underwent multimodal MRI scans at T0 and T2 (see *Image acquisition* below); only dMRI and rsfMRI scans at T0 are analysed in this study.

2.3. Image acquisition

Participants were scanned on a GE Signa HDxT 3 T MRI scanner using a 32-channel head coil (General Electric, Milwaukee, U.S). Anatomical MRI was acquired using a 3D T1-weighted structural magnetization-prepared rapid acquisition gradient-echo (MPRAGE; TR = 6.9 ms; TI = 900 ms; TE = 3.0 ms; 256x256 matrix; 1 mm3 isotropic resolution; 168 sections) and was used for coregistration and normalisation of fMRI and dMRI scans. All rsfMRI scans were acquired using a gradient echo-planar imaging sequence (TR = 2.2 s; TE = 26 ms; 64x64 matrix; field of view 21.1 cm; flip angle = 80°) with 275 volumes and 42 ascending slices per volume (3.3 x 3.3 mm in-plane resolution; slice thickness = 3.0 mm; interslice gap = 0.3 mm). Participants were scanned in a darkened room, and were instructed to remain awake with their eyes closed during the scan (10 min in total). DMRI multi-shell images consisted of 73 diffusion-weighted directions (25 b1000, 24 b2000, and 24 b3000 s/mm^2) and seven interleaved non-diffusion-weighted volumes (b0 s/mm^2). Additional fieldmaps (for both the rsfMRI and dMRI) were acquired with opposite phase-encoding directions for distortion correction.

2.4. rsfMRI processing

RsfMRI data were pre-processed using fMRIprep v21.0.1 (https://fmriprep.org) (see Supplement for boilerplate). In fMRIprep, reversed phase-encoding scans were used to account for susceptibility-induced distortions, volume alignment was carried out, and motion parameters were extracted. Additional steps included motion correction (performed using Automatic Removal of Motion Artifacts and Independent Component Analysis (ICA-AROMA) (Pruim et al., 2015) and regressing out sources of physiological noise from grey and white matter), 0.009–0.08 Hz bandpass filtering, and 6 mm smoothing using FSL SUSAN (Smith and Brady, 1997). Parcellation of each participant's T1-weighted image was carried out using the Schaefer 300 cortical atlas (Schaefer et al., 2018) plus 14 subcortical regions individually segmented using FreeSurfer (v7.1.1) (Desikan et al., 2006). This was followed by extraction of average BOLD-signals from each brain area. The z-transformed, absolutised Pearson correlations between each node's timeseries formed the weighted edges of the functional network.

2.5. dMRI processing

Diffusion images were denoised using the *dwidenoise* tool in MRtrix3 (Tournier et al., 2019), and corrected for eddy currents, susceptibility-induced distortions, and within- and between-volume motion using eddy from the FMRIB Software Library (FSL; v6.0.5). We used eddyqc (Bastiani et al., 2019) to extract image quality measures. Outliers were visually inspected to identify volumes with residual (motion-related) artefacts and deleted if necessary. Structural connectomes were constructed using probabilistic anatomically-constrained tractography (ACT) (Smith et al., 2012) in MRtrix3 (Tournier et al., 2019). Tissue response function estimation was carried out using the multishell multitissue five-tissue-type algorithm (msmt_5tt), followed by multishell multitissue constrained spherical deconvolution (MSMT-CSD) (Jeurissen et al., 2014). Tractograms were constructed by random seeding of 50 million fibres at the grey matter/white matter boundary, followed by spherical-deconvolution informed filtering of tractograms (SIFT2 from MRtrix3) (Smith et al., 2015). Finally, the above parcellation of each participant's T1-weighted image was used to convert the tractogram to a structural network, where weighted links represented streamline counts between all voxels within two brain regions.

2.6. Parcellation and definition of whole-brain atlas, stimulated node and subnetwork

Due to signal loss in the rsfMRI data, we were not able to retain all atlas regions; for our analyses we used the subset of atlas nodes common to both the structural and functional data of all participants. Our final atlas consisted of 307 nodes (we excluded 7 nodes in bilateral orbital frontal cortex and bilateral temporal pole: see Supplement for specific regions).

Stimulated nodes were defined as the atlas region that overlapped most with a 5 mm radius sphere constructed around the stimulated rTMS coordinates in MNI space. For the vertex group, the DLPFC and preSMA coordinates were defined in the same way as in the DLPFC and preSMA groups to act as control comparison coordinates (further referred to as vertex-DLPFC and vertex-preSMA, respectively), but these participants were not stimulated at these locations. The stimulated subnetwork was defined as the Yeo 7-network subdivision (Yeo et al., 2011) containing the stimulated node. We chose to use Yeo's 7-network parcellation of resting state networks to define stimulated subnetworks; these networks are stable and reproducible across participants (Yeo et al., 2011), and may also be relevant for clinical rTMS effects (Rosen et al., 2021). If shown to be related to rTMS outcome, they may also provide a reproducible and easily identifiable target for use in clinical rTMS application.

2.7. Graph analyses and network measure extraction

Single-layer networks: Weighted networks were constructed for both structural and functional data. The following graph measures were calculated using the Brain Connectivity Toolbox (BCT) (Rubinov and Sporns, 2010) (https://sites.google.com/site/bctnet/):

- Nodal measures: node strength (NS), betweenness centrality (BC), participation coefficient (PC) and eigenvector centrality (EC) (see Box 1) of stimulated and hypothetical stimulated nodes in rsfMRI and dMRI networks
- Subnetwork measures: NS, BC, PC and EC of all nodes in each stimulated and hypothetically stimulated Yeo subnetwork and averaged across the subnetwork.

Box 1: Graph measure definitions.

- Node strength – the total strength of a nodés connections, or how strongly connected a node is to its neighbours. Can be considered a measure of local connectivity (Rubinov and Sporns, 2010).
- Degree centrality – the equivalent of node strength for binarised networks: the number of connections a node has.
- Betweenness centrality – measures how many high strength paths in the network pass through a node, giving a measure of global connectivity (connectivity throughout the entire network) (Rubinov and Sporns, 2010).
- Participation coefficient – a high participation coefficient indicates a relatively high number of connections outside compared to within a node's subnetwork (Sporns, 2014).

Eigenvector centrality – denotes the influence of a node in a network – high EC nodes have connections with nodes that also connect with highly central nodes (Lohmann et al., 2010).

Multilayer networks: Binary multiplex networks were constructed, using the same in-house scripts as Breedt et al 2023 (Breedt et al., 2023) (https://github.com/multinetlab-amsterdam/projects/tree/master/mumo_paper_2021), with two layers consisting of 1) a functional, rsfMRI-derived minimum spanning tree (MST) network 2) a structural, dMRI-derived MST network. MSTs are binarised networks, formed from the strongest links of the weighted version of the network, that connect

Table 1
Demographic and clinical information.

	Overall (N = 58)	DLPFC (N = 19)	preSMA (N = 21)	vertex (N = 18)	Comparison
Demographic data					
Sex, n (%)					
male	20 (34.5%)	6 (31.6%)	9 (42.9%)	5 (27.8%)	$\chi^2(2) = 1.081$,
female	38 (65.5%)	13 (68.4%)	12 (57.1%)	13 (72.2%)	$p = 0.583$[a]
Age					
Mean (SD)	36.4 (12.7)	40.3 (12.4)	30.3 (12.7)	39.3 (10.7)	**H(2) = 11.031, p = 0.004**[b]
Education[d]					
Median [Min, Max]	9.00 [4.00, 10.0]	9.00 [4.00, 10.0]	9.00 [4.00, 10.0]	9.00 [6.00, 10.0]	H(2) = 0.615, p = 0.735[b]
Clinical data					
Age of symptom onset					
Mean (SD)	15.4 (7.88)	15.8 (8.43)	15.5 (7.52)	15.1 (8.09)	H(2) = 0.041, p = 0.979[b]
Medication status n (%)					
unmedicated	23 (39.7%)	5 (26.3%)	8 (38.1%)	10 (55.6%)	$\chi^2(2) = 2.758$,
medicated	35 (60.3%)	14 (73.7%)	13 (61.9%)	8 (44.4%)	$p = 0.250$[a]
T0 YBOCS score					
Mean (SD)	28.2 (4.68)	28.8 (5.68)	29.4 (3.47)	26.3 (4.35)	F = 2.517, p = 0.090[c]
Response status at T2 n (%)					
nonresponder	25 (43.1%)	7 (36.8%)	11 (52.4%)	7 (38.9%)	$\chi^2(2) = 1.171$,
responder	33 (56.9%)	12 (63.2%)	10 (47.6%)	11 (61.1%)	$p = 0.557$[a]
T0 BDI score					
Mean (SD)	18.7 (10.7)	22.0 (11.3)	21.6 (10.7)	11.8 (6.48)	**H(2) = 11.555, p = 0.003**[b]
Comorbidities (n, %)					
Depressive disorder	11 (19.0%)	4 (21.1%)	7 (33.3%)	0 (0%)	**$\chi^2(2) = 7.087$, p = 0.029**[a]
ADHD	6 (10.3%)	2 (10.5%)	2 (9.5%)	2 (11.1%)	$\chi^2(2) = 0.027$, p = 0.986[a]
General anxiety disorder	5 (8.6%)	3 (15.8%)	1 (4.8%)	1 (5.6%)	$\chi^2(2) = 0.986$, p = 0.396[a]
Panic disorder	2 (3.4%)	1 (5.3%)	0 (0%)	1 (5.6%)	$\chi^2(2) = 1.178$, p = 0.555[a]
Specific phobia	2 (3.4%)	2 (10.5%)	0 (0%)	0 (0%)	$\chi^2(2) = 4.252$, p = 0.119[a]
Alcohol use disorder	2 (3.4%)	1 (5.3%)	1 (4.8%)	0 (0%)	$\chi^2(2) = 0.940$, p = 0.625[a]
Social anxiety disorder	1 (1.7%)	1 (5.3%)	0 (0%)	0 (0%)	$\chi^2(2) = 2.089$, p = 0.352[a]
Body dysmorphic disorder	1 (1.7%)	0 (0%)	0 (0%)	1 (5.6%)	$\chi^2(2) = 2.261$, p = 0.323[a]
Anorexia nervosa	1 (1.7%)	1 (5.3%)	0 (0%)	0 (0%)	$\chi^2(2) = 2.089$, p = 0.352[a]
PTSD	1 (1.7%)	0 (0%)	1 (4.8%)	0 (0%)	$\chi^2(2) = 1.793$, p = 0.408[a]

a = chi-squared test; b = kruskal–wallis test; c = one-way anova; d. Level of education expressed as a 9 point scale, with: 1 = no finished education, 9 = university.. ADHD, attention-deficit/hyperactivity disorder; BDI, Beck Depression Index; DLPFC, dorsolateral prefrontal cortex; preSMA, pre-supplementary motor area; PTSD, post-traumatic stress disorder; rTMS, repetitive transcranial magnetic stimulation; SD, standard deviation; SRI, serotonin reuptake inhibitors; T0, baseline; YBOCS, Yale-Brown Obsessive Compulsive Scale.

all nodes in the network with a link of weight = 1 without forming loops. Graph measures calculated from MSTs have the advantage of not being influenced by connection strength or link density, while remaining similar to measures calculated from the original underlying network (Tewarie et al., 2015). We chose to use MST for our multilayer networks so that there would not be differences in link density in the different layers. Interlayer links were present only between the same nodes across layers (with weight = 1).

The following graph measures were calculated:

- Nodal measures: degree centrality (DC), BC, and EC of stimulated and hypothetical stimulated nodes in multilayer networks were extracted using in-house scripts (https://github.com/multinetlab-amsterdam/data_analysis/tree/Multilayer/Multilayer).
- Subnetwork measures: DC, BC, and EC of all nodes in each stimulated and hypothetically stimulated Yeo subnetwork were extracted and averaged across the subnetwork.

2.8. Statistical analyses

Analyses were pre-registered at https://osf.io/s9krj. All statistical analyses were performed in R (v4.2.1, Vienna, Austria).

Primary outcome: We performed linear regression analyses to statistically test the association between baseline graph measures and treatment response, as defined by pre-post treatment change in YBOCS score (ΔYBOCS). The node and subnetwork graph measures NS, BC, PC, and EC in structural and functional single-layer networks, and DC, BC, and EC for multilayer networks, were included in separate models as the dependent variable. The independent variable was defined as ΔYBOCS, with covariates age, sex and baseline YBOCS, to allow us to accurately calculate and control for the effect of baseline YBOCS on ΔYBOCS. Analyses were performed for each group separately (DLPFC, preSMA, vertex-DLPFC, vertex-preSMA). To correct for multiple tests, and since graph measures are highly correlated, we used a Sidak/D-AP-corrected alpha of 0.019 for the single layer networks and 0.025 for the multilayer networks, calculated via the SISA website (Uitenbroek, 1997) based on the average correlation between the graph measures (r = 0.301 for single-layer networks, r = 0.361 for multilayer networks). Given the exploratory nature of these analyses, we chose to only correct across graph measures. We also performed these analyses in all groups combined in order to examine general associations with treatment outcome.

Exploratory outcomes: Because the preSMA and DLPFC coordinates were individually determined, different Yeo resting state subnetworks (Yeo et al., 2011) were stimulated in each participant. We therefore examined whether symptom improvement following rTMS was dependent on the subnetwork that the stimulated node happened to occur in. Participants in the preSMA and DLPFC groups were combined and then regrouped according to which Yeo subnetwork was stimulated. ΔYBOCS was compared between stimulated Yeo subnetworks using a *t*-test and responder rates using a chi-squared test. Subnetworks containing the hypothetically stimulated nodes in the vertex group were compared separately as a control. Demographic characteristics were compared between groups using one-way ANOVAs, chi-squared tests, or Kruskal-Wallace tests as appropriate. ΔYBOCS over time was compared between groups using linear mixed models (see also (Fitzsimmons et al., 2023).

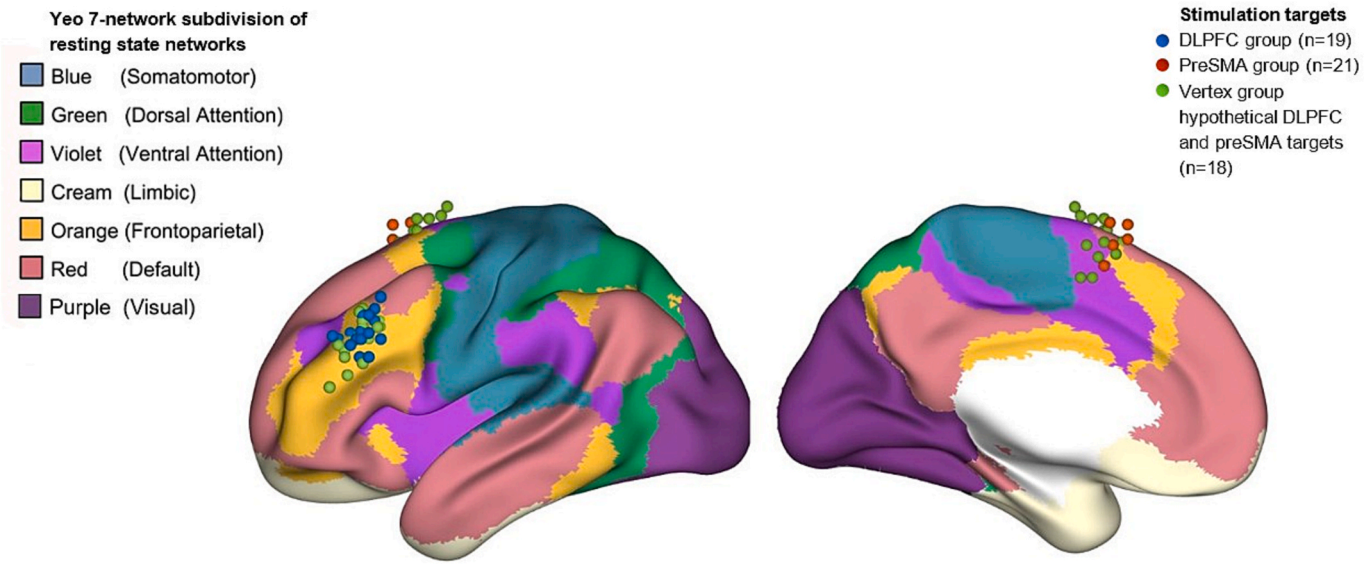

Fig. 1. Lateral (left) and medial (right) view of rTMS stimulation locations and their localisation within Yeo 7-network subdivision of resting state networks. Dorsolateral prefrontal cortex (DLPFC) group stimulation targets (n = 19) in blue; pre-supplementary motor area (preSMA) group (n = 21) in red; hypothetical preSMA and DLPFC stimulation targets for vertex group (n = 18) in light green. (For interpretation of the references to colour in this figure legend, the reader is referred to the web version of this article.)

3. Results

3.1. Demographic information

Of the 64 participants that started treatment, three participants dropped out during treatment and lacked clinical data at T2, two did not have rsfMRI/dMRI scans available, and one was excluded due to lack of fMRI signal at the stimulation location. Fifty-eight had usable rsfMRI/dMRI data at T0 and clinical measurements at both T0 and T2 and are included in the present study (19 in the DLPFC group, 21 in the preSMA group, 18 in the vertex group). Clinical and demographic details are presented in Table 1. Groups were generally well-matched across demographic and baseline clinical characteristics, though the preSMA group was significantly younger than the other groups ($p = 0.004$). The vertex group had a lower Beck Depression Index (BDI) score than the other groups ($p = 0.003$), and lower rates of comorbid depression ($p = 0.029$).

3.2. Clinical outcomes

Full clinical outcomes are reported elsewhere (Fitzsimmons et al., 2023). Symptom severity decreased significantly at T2 compared to T0 (T0-T2 mean difference = -10.836, $p < 0.001$, 95% CI [-12.504, −9.168])). There was no statistically significant group by time interaction, both before and after adjusting for age, sex, and baseline BDI, indicating no group differences in symptom reduction.

3.3. Distribution of stimulation locations

See Fig. 1 and Table S1 in the Supplement for a visualisation of the stimulation locations and the stimulated Yeo resting state networks. The stimulation location for the majority of the DLPFC group was in the frontoparietal network (FPN, 14/19) while for the preSMA group this was the default mode network (DMN, 16/21). There was no significant difference in symptom improvement (ΔYBOCS) ($t(37) = 1.01$, $p = 0.318$) or number of responders ($\chi^2(1) = 0.710$, $p = 0.400$) between those stimulated in the FPN and those stimulated in the DMN.

3.4. Association of treatment outcome with single-layer network properties

Following correction for multiple comparisons, no single-layer structural or functional graph features were associated with treatment outcome in either active rTMS or vertex groups (See Supplementary tables S2 and S3 for multiple regression results). We also found no significant associations between graph features and treatment outcome in all participants combined for either type of single-layer network.

3.5. Association of treatment outcome with multilayer network properties

Greater multilayer BC of the stimulated subnetwork was associated with greater symptom improvement following DLPFC rTMS ($p = 0.013$, Fig. 2, table S4), while multilayer BC of the equivalent hypothetical DLPFC network in the vertex group was not associated with treatment outcome ($p = 0.143$, Fig. 2, table S4). Multilayer BC of the stimulated subnetwork in the preSMA group was also not associated with treatment outcome ($p = 0.639$, Fig. 2, table S4). No other associations between stimulation location or stimulated network graph features and treatment outcome survived correction for multiple comparisons (table S4). We found no significant associations between multilayer graph features of the stimulated region and treatment outcome in all participants combined.

In order to check whether association of BC with treatment outcome was specific to the stimulated networks, and not in the whole brain or unstimulated networks, we carried out further post hoc analyses within the DLPFC group. We calculated the association of treatment outcome with mean whole brain BC, mean whole brain BC without FPN and DMN, and mean sensorimotor network BC for the DLPFC group (Table S5). None were significantly associated with treatment outcome.

4. Discussion

We investigated the relationship between single- and multilayer structural and functional brain network properties of the stimulation location and treatment outcome of a combined rTMS and ERP treatment for OCD. No associations were found between functional or structural single-layer graph metrics and treatment outcome for any group. For combined rTMS and ERP of the DLPFC, greater structural–functional

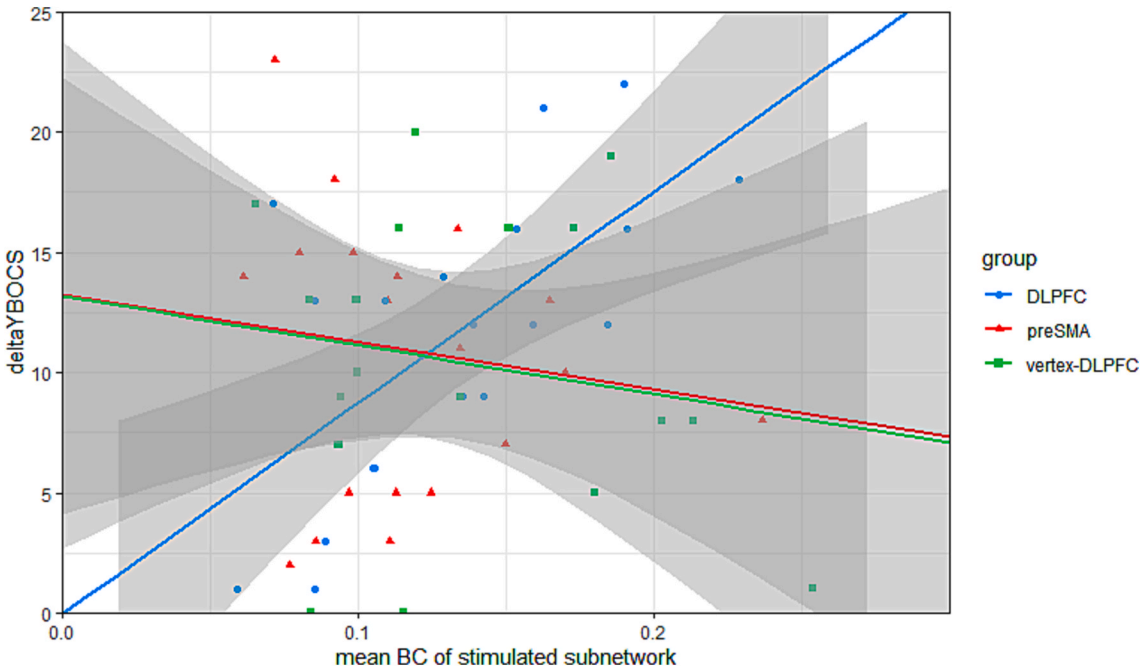

Fig. 2. Scatterplot showing association of meanbetweenness centrality (BC) of stimulated multilayer subnetwork (i.e. the Yeo subnetwork containing the stimulated node) with change in YBOCS scores in DLPFC group (blue), preSMA group (red), and the hypothetical DLPFC-related network for the vertex group (green). (For interpretation of the references to colour in this figure legend, the reader is referred to the web version of this article.)

multilayer BC of the stimulated subnetwork was associated with increased symptom improvement following treatment. This relationship was not observed in the equivalent DLPFC subnetwork in the vertex group, or in the stimulated subnetwork in the preSMA group.

Our exploratory findings indicate that structural–functional multilayer connectivity of the stimulated subnetwork may be a determinant of high frequency DLPFC rTMS combined with ERP in OCD: the more well integrated the stimulated subnetwork is with the rest of the brain, the greater the symptom improvement. The direction of effect is contrary to our hypothesised effect – we expected that lower global and higher local connectivity would be correlated with greater treatment effect. Contrary to our other hypothesis, we did not observe an association with rTMS effect in the single-layer networks, while in our previous work on the functional single-layer brain network in healthy subjects (Fitzsimmons et al., 2020) and OCD (Douw et al., 2020), we did find centrality measures that were related to rTMS outcome. One possible explanation for these observations is that these earlier studies were based on single-session *'experimental'* rTMS, while the current study examines multi-session *'therapeutic'* rTMS. There may be fundamental differences in working mechanisms between single and multi-session rTMS: a systematic review by Beynel et al (Beynel et al., 2020) observed that single sessions of rTMS generally led to mixed increases and decreases in rsfMRI FC, while multiple sessions tended to lead to increases in FC, regardless of the stimulation frequency. This may be due to differences in plasticity mechanisms between single session and multisession rTMS, with changes following single sessions possibly reflecting short term plasticity, and following multisession rTMS compensatory/homeostatic plasticity (Zhong et al., 2021; Michael et al., 2003; Karabanov et al., 2015). Additionally, the current study examined a combined rTMS-ERP treatment, which may also have different working mechanisms than rTMS without psychotherapy.

Interestingly, we did not observe a relationship between mean multilayer betweenness centrality of the stimulated subnetwork and treatment outcome in the preSMA-stimulated group. One possible explanation for this may lie in differences in rTMS dosing between the groups. A recently performed Efield analysis of this dataset shows that the preSMA group was underdosed compared to the DLPFC group; and the distance from coil to target and coil to brain surface was also greater at this location compared to the DLPFC group (unpublished data, manuscript submitted). This may point to a reduced or inconsistent influence of the rTMS on the preSMA target region and may explain the lack of association in this group.

Another difference between the DLPFC and preSMA groups lay in the most frequently stimulated resting state subnetwork per group: in the DLPFC group this was the FPN, in the preSMA group the DMN. One study of DLPFC rTMS stimulation locations for the treatment for depression found that stimulation locations of responders had greater FC with the FPN, while the stimulation locations of nonresponders had greater FC with the DMN (Rosen et al., 2021). However, since our own analyses showed no difference in response rates between those stimulated at the FPN vs the DMN, we cannot be certain whether this difference has affected our results.

Our results show an association between the BC of the stimulated subnetwork and treatment outcome in the DLPFC-stimulated group, regardless of which resting state network was actually stimulated. We specifically found that average betweenness centrality across the subnetwork, (which represents good integration of the subnetwork with the rest of the brain), was associated with treatment outcome. It may therefore be the case that it is not the function of the stimulated network that is important, but its connectivity to the rest of the brain. A well-connected stimulated subnetwork may allow better transmission of rTMS-induced plasticity (most FC changes following rTMS are found in distant regions rather than in the stimulated area (Beynel et al., 2020). In the case of this specific trial, it may allow better synergy with exposure therapy plasticity effects (CBT in OCD and other psychiatric disorders has been shown to have effects throughout the brain such as as higher visual areas, not just within the prefrontal cortex or cognitive control/default mode networks (Li et al., 2018; Machado-Sousa et al., 2025; Yuan et al., 2022). The network effects of rTMS may also be the reason that treatment outcome was associated with BC of the stimulated subnetwork but not BC of the stimulated node: connectivity properties of the stimulated subnetwork capture the network-wide influence of rTMS better than the connectivity properties of only the stimulated node.

Our research gives an indication that neither structural nor

functional connectivity alone, but rather the combined contribution of structural and functional networks is important for the efficacy of multi-session rTMS. Other research has also suggested that this interplay may be an important determinant of rTMS effects. TMS pulses have been shown to preferentially propagate via anatomical pathways of the structural network over those of the functional network (Momi et al., 2021), while at the same time a broad range of approaches and analyses indicate that the connectivity of the functional brain network is an important predictor of rTMS effect (Fox et al., 2012; Cash et al., 2019; Weigand et al., 2018). An integrative metric that combines these two brain features may allow a better representation of the complex relationship of both brain structure and function to brain stimulation outcome. For example, a study (Lai et al., 2023) of deep brain stimulation in depression found that a combined functional and structural connectivity mask predicted treatment outcome better than either functional or structural connectivity alone.

Our study has a number of weaknesses. As discussed in the primary outcomes paper for this trial (Fitzsimmons et al., 2023), since we used low intensity active stimulation at the vertex, we cannot rule out the possibility that we induced some parietal stimulation during the treatment which may have had a therapeutic effect. The vertex condition is therefore an imperfect placebo; this finding requires replication with a true sham condition as a comparator. Our sample size per group is also relatively small: we may have failed to detect associations with the single-layer networks due to a lack of power (though the fact that we do detect an effect with multilayer networks with a small sample size and correction for multiple comparisons suggests that multilayer may be more sensitive to rTMS effects than single-layer). We acknowledge, however, that the p-value of our main finding is borderline and might not survive more aggressive correction for multiple comparisons. Our chosen correction approach across graph measures (Sidak/D-AP-corrected alpha, corrected for correlations between graph measures), but not across groups, balances protection against false positives with the preservation of statistical power to detect meaningful effects, following methodological recommendations (Rothman, 1990; Streiner and Norman, 2011; Feise, 2002) that the definition of a correction family should be guided by the research hypotheses rather than the total number of statistical tests performed. Additionally, the effect size of the finding (adjusted R^2 0.39) is moderate to large. While the effect may be somewhat inflated given the small sample size, it indicates the likely presence of an association which requires further investigation in an adequately powered sample. Taken together, this result should be interpreted as an exploratory result warranting replication rather than as definitive evidence.

Our study also has several strengths. To our knowledge, this is the first study to examine the association between multilayer networks and rTMS effect, and one of few that examine the relationship between integrated structural and functional neuroimaging data and rTMS treatment outcomes. We use MST networks to construct our multilayer networks, removing potential bias related to link density or average connectivity (Mandke et al., 2018).

Multilayer networks may offer a useful method to predict rTMS outcome and plan future treatments. Identifying properties of the stimulation location that are associated with greater treatment response may help improve selection of rTMS target sites. However, the true added value of this complex and labour-intensive approach needs to be evaluated before implementation in the clinic could be considered for response prediction and/or optimised targeting – a recent randomised trial (Morriss et al., 2024) indicated that neuronavigation based on FC defined targets has limited added value over anatomical targeting.

In conclusion, we found that while structural and functional single-layer network properties were not associated with treatment outcome of rTMS-ERP for OCD, participants with greater multilayer BC of the stimulated subnetwork (greater integration of the stimulated subnetwork with the rest of the structural–functional network) showed greater improvement following DLPFC rTMS-ERP. Our exploratory results give a preliminary indication that the outcome of rTMS-ERP treatment for OCD is dependent on the combined contribution of structural and functional networks, and that multilayer network analysis may be a useful tool for future rTMS research.

CRediT authorship contribution statement

Sophie M.D.D. Fitzsimmons: Writing – review & editing, Writing – original draft, Formal analysis, Conceptualization. **Coen Coomans:** Writing – review & editing, Formal analysis, Data curation. **Lucas Breedt:** Writing – review & editing, Formal analysis. **Neeltje M. Batelaan:** Writing – review & editing, Supervision, Conceptualization. **Ysbrand D. van der Werf:** . **Odile A. van den Heuvel:** Writing – review & editing, Supervision, Conceptualization. **Linda Douw:** Writing – review & editing, Supervision, Methodology, Formal analysis, Conceptualization. **Chris Vriend:** Writing – review & editing, Supervision, Formal analysis, Conceptualization.

Declaration of Competing Interest

The authors declare that they have no known competing financial interests or personal relationships that could have appeared to influence the work reported in this paper.

Acknowledgements

This work was supported by a NWO-ZonMw VIDI grant (016.176.306) awarded to OAvdH, and a NWO VIDI grant (198.015) awarded to LD.

Appendix A. Supplementary data

Supplementary data to this article can be found online at https://doi.org/10.1016/j.nicl.2026.104012.

Data availability

The authors do not have permission to share data.

References

Hyde, J., Carr, H., Kelley, N., Seneviratne, R., Reed, C., Parlatini, V., et al., 2022. Efficacy of neurostimulation across mental disorders: systematic review and meta-analysis of 208 randomized controlled trials. Mol. Psychiatry 27, 2709–2719. https://doi.org/10.1038/s41380-022-01524-8.

Kan, R.L.D., Padberg, F., Giron, C.G., Lin, T.T.Z., Zhang, B.B.B., Brunoni, A.R., et al., 2023. Effects of repetitive transcranial magnetic stimulation of the left dorsolateral prefrontal cortex on symptom domains in neuropsychiatric disorders: a systematic review and cross-diagnostic meta-analysis. Lancet Psychiatry 10, 252–259. https://doi.org/10.1016/S2215-0366(23)00026-3.

Lefaucheur, J.-P., Aleman, A., Baeken, C., Benninger, D.H., Brunelin, J., Di Lazzaro, V., et al., 2020. Evidence-based guidelines on the therapeutic use of repetitive transcranial magnetic stimulation (rTMS): an update (2014-2018). Clin. Neurophysiol. 131, 474–528. https://doi.org/10.1016/j.clinph.2019.11.002.

Siebner, H.R., Funke, K., Aberra, A.S., Antal, A., Bestmann, S., Chen, R., et al., 2022. Transcranial magnetic stimulation of the brain: what is stimulated? – a consensus and critical position paper. Clin. Neurophysiol. 140, 59–97. https://doi.org/10.1016/j.clinph.2022.04.022.

Fitzsimmons, S.M.D.D., Oostra, E., Postma, T.S., van der Werf, Y.D., van den Heuvel, O. A., 2024. Repetitive Transcranial magnetic Stimulation-Induced Neuroplasticity and the Treatment of Psychiatric Disorders: State of the evidence and Future Opportunities. Biol. Psychiatry 95, 592–600. https://doi.org/10.1016/j.biopsych.2023.11.016.

Fox, M.D., Buckner, R.L., White, M.P., Greicius, M.D., Pascual-Leone, A., 2012. Efficacy of Transcranial magnetic Stimulation Targets for Depression is Related to Intrinsic Functional Connectivity with the Subgenual Cingulate. Biol. Psychiatry 72, 595–603. https://doi.org/10.1016/j.biopsych.2012.04.028.

Cash, R.F.H., Zalesky, A., Thomson, R.H., Tian, Y., Cocchi, L., Fitzgerald, P.B., 2019. Subgenual Functional Connectivity Predicts Antidepressant Treatment Response to Transcranial magnetic Stimulation: Independent Validation and Evaluation of Personalization. Biol. Psychiatry 86, e5–e7. https://doi.org/10.1016/j.biopsych.2018.12.002.

Cash, R.F.H., Cocchi, L., Lv, J., Wu, Y., Fitzgerald, P.B., Zalesky, A., 2021. Personalized connectivity-guided DLPFC-TMS for depression: advancing computational feasibility, precision and reproducibility. Hum. Brain Mapp. 42, 4155–4172. https://doi.org/10.1002/hbm.25330.

Weigand, A., Horn, A., Caballero, R., Cooke, D., Stern, A.P., Taylor, S.F., et al., 2018. Prospective Validation that Subgenual Connectivity Predicts Antidepressant Efficacy of Transcranial magnetic Stimulation Sites. Biol. Psychiatry 84, 28–37. https://doi.org/10.1016/j.biopsych.2017.10.028.

Klooster, D.C.W., Vos, I.N., Caeyenberghs, K., Leemans, A., David, S., Besseling, R.M.H., et al., 2020. Indirect frontocingulate structural connectivity predicts clinical response to accelerated rTMS in major depressive disorder. J. Psychiatry Neurosci. 45, 243–252. https://doi.org/10.1503/jpn.190088.

Barredo, J., Bellone, J.A., Edwards, M., Carpenter, L.L., Correia, S., Philip, N.S., 2019. White matter integrity and functional predictors of response to repetitive transcranial magnetic stimulation for posttraumatic stress disorder and major depression. Depress. Anxiety 36, 1047–1057. https://doi.org/10.1002/da.22952.

Ning, L., Rathi, Y., Barbour, T., Makris, N., Camprodon, J.A., 2022. White matter markers and predictors for subject-specific rTMS response in major depressive disorder. J. Affect. Disord. 299, 207–214. https://doi.org/10.1016/J.JAD.2021.12.005.

Bullmore, E., Sporns, O., 2009. Complex brain networks: graph theoretical analysis of structural and functional systems. Nat. Rev. Neurosci. 10, 186–198. https://doi.org/10.1038/nrn2575.

Fornito A, Zalesky A, Bullmore ET, editors. Chapter 5 - Centrality and Hubs. Fundamentals of Brain Network Analysis, San Diego: Academic Press; 2016, p. 137–61. https://doi.org/10.1016/B978-0-12-407908-3.00005-4.

Fitzsimmons, S.M.D.D., Douw, L., van den Heuvel, O.A., van der Werf, Y.D., Vriend, C., 2020. Resting-state and task-based centrality of dorsolateral prefrontal cortex predict resilience to 1 Hz repetitive transcranial magnetic stimulation. Hum. Brain Mapp. 41, 3161–3171. https://doi.org/10.1002/hbm.25005.

Douw, L., Quaak, M., Fitzsimmons, S.M.D.D., de Wit, S.J., van der Werf, Y.D., van den Heuvel, O.A., et al., 2020. Static and dynamic network properties of the repetitive transcranial magnetic stimulation target predict changes in emotion regulation in obsessive-compulsive disorder. Brain Stimul. 13, 318–326. https://doi.org/10.1016/j.brs.2019.10.017.

Honey, C.J., Kötter, R., Breakspear, M., Sporns, O., 2007. Network structure of cerebral cortex shapes functional connectivity on multiple time scales. PNAS 104, 10240–10245. https://doi.org/10.1073/pnas.0701519104.

Deco, G., Jirsa, V.K., McIntosh, A.R., 2011. Emerging concepts for the dynamical organization of resting-state activity in the brain. Nat. Rev. Neurosci. 12, 43–56. https://doi.org/10.1038/nrn2961.

Honey, C.J., Sporns, O., Cammoun, L., Gigandet, X., Thiran, J.P., Meuli, R., et al., 2009. Predicting human resting-state functional connectivity from structural connectivity. PNAS 106, 2035–2040. https://doi.org/10.1073/pnas.0811168106.

Breedt, L.C., Santos, F.A.N., Hillebrand, A., Reneman, L., van Rootselaar, A.-F., Schoonheim, M.M., et al., 2023. Multimodal multilayer network centrality relates to executive functioning. Netw Neurosci 7, 299–321. https://doi.org/10.1162/netn_a_00284.

de Kwaasteniet, B., Ruhe, E., Caan, M., Rive, M., Olabarriaga, S., Groefsema, M., et al., 2013. Relation between structural and functional connectivity in major depressive disorder. Biol. Psychiatry 74, 40–47. https://doi.org/10.1016/j.biopsych.2012.12.024.

De Domenico, M., 2017. Multilayer modeling and analysis of human brain networks. GigaScience 6, gix004. https://doi.org/10.1093/gigascience/gix004.

Battiston, F., Nicosia, V., Chavez, M., Latora, V., 2017. Multilayer motif analysis of brain networks. Chaos 27, 047404. https://doi.org/10.1063/1.4979282.

Simas, T., Chavez, M., Rodriguez, P.R., Diaz-Guilera, A., 2015. An algebraic topological method for multimodal brain networks comparisons. Front. Psychol. 6, 904. https://doi.org/10.3389/fpsyg.2015.00904.

Guillon, J., Attal, Y., Colliot, O., La Corte, V., Dubois, B., Schwartz, D., et al., 2017. Loss of brain inter-frequency hubs in Alzheimer's disease. Sci. Rep. 7, 10879. https://doi.org/10.1038/s41598-017-07846-w.

De Domenico, M., Sasai, S., Arenas, A., 2016. Mapping Multiplex Hubs in Human Functional Brain Networks. Front. Neurosci. 10, 326. https://doi.org/10.3389/fnins.2016.00326.

van Lingen, M.R., Breedt, L.C., Geurts, J.J.G., Hillebrand, A., Klein, M., Kouwenhoven, M.C.M., et al., 2023. The longitudinal relation between executive functioning and multilayer network topology in glioma patients. Brain Imaging Behav. 17, 425–435. https://doi.org/10.1007/s11682-023-00770-w.

Fitzsimmons SMDD, Postma T, van Campen AD, Vriend C, Bateaan NM, van Oppen P, et al. TMS-induced plasticity improving cognitive control in OCD I: Clinical and neuroimaging outcomes from a randomised trial of rTMS for OCD. medRxiv 2023: 2023.11.04.23298100. https://doi.org/10.1101/2023.11.04.23298100.

Vázquez-Rodríguez, B., Suárez, L.E., Markello, R.D., Shafiei, G., Paquola, C., Hagmann, P., et al., 2019. Gradients of structure–function tethering across neocortex. Proc. Natl. Acad. Sci. 116, 21219–21227. https://doi.org/10.1073/pnas.1903403116.

First M, Williams J, Karg R, Spitzer R. Structured Clinical Interview for DSM-5 Disorders, Clinician Version (SCID-5-CV). Arlington, VA: American Psychiatric Association; 2016.

Goodman, W.K., Price, L.H., Rasmussen, S.A., Mazure, C., Fleischmann, R.L., Hill, C.L., et al., 1989. The Yale-Brown Obsessive Compulsive Scale. I. Development, use, and reliability. Arch. Gen. Psychiatry 46, 1006–1011. https://doi.org/10.1001/archpsyc.1989.01810110048007.

Pruim, R.H.R., Mennes, M., Van Rooij, D., Llera, A., Buitelaar, J.K., Beckmann, C.F., 2015. ICA-AROMA: a robust ICA-based strategy for removing motion artifacts from fMRI data. Neuroimage 112, 267–277. https://doi.org/10.1016/j.neuroimage.2015.02.064.

Smith, S.M., Brady, J.M., 1997. SUSAN—A New Approach to Low Level image Processing. Int. J. Comput. Vis. 23, 45–78. https://doi.org/10.1023/A:1007963824710.

Schaefer, A., Kong, R., Gordon, E.M., Laumann, T.O., Zuo, X.-N., Holmes, A.J., et al., 2018. Local-Global Parcellation of the Human Cerebral Cortex from Intrinsic Functional Connectivity MRI. Cereb. Cortex 28, 3095–3114. https://doi.org/10.1093/cercor/bhx179.

Desikan, R.S., Ségonne, F., Fischl, B., Quinn, B.T., Dickerson, B.C., Blacker, D., et al., 2006. An automated labeling system for subdividing the human cerebral cortex on MRI scans into gyral based regions of interest. Neuroimage 31, 968–980. https://doi.org/10.1016/j.neuroimage.2006.01.021.

Tournier, J.-D., Smith, R., Raffelt, D., Tabbara, R., Dhollander, T., Pietsch, M., et al., 2019. MRtrix3: a fast, flexible and open software framework for medical image processing and visualisation. Neuroimage 202, 116137. https://doi.org/10.1016/j.neuroimage.2019.116137.

Bastiani, M., Cottaar, M., Fitzgibbon, S.P., Suri, S., Alfaro-Almagro, F., Sotiropoulos, S.N., et al., 2019. Automated quality control for within and between studies diffusion MRI data using a non-parametric framework for movement and distortion correction. Neuroimage 184, 801–812. https://doi.org/10.1016/j.neuroimage.2018.09.073.

Smith, R.E., Tournier, J.-D., Calamante, F., Connelly, A., 2012. Anatomically-constrained tractography: improved diffusion MRI streamlines tractography through effective use of anatomical information. Neuroimage 62, 1924–1938. https://doi.org/10.1016/j.neuroimage.2012.06.005.

Jeurissen, B., Tournier, J.-D., Dhollander, T., Connelly, A., Sijbers, J., 2014. Multi-tissue constrained spherical deconvolution for improved analysis of multi-shell diffusion MRI data. Neuroimage 103, 411–426. https://doi.org/10.1016/j.neuroimage.2014.07.061.

Smith, R.E., Tournier, J.-D., Calamante, F., Connelly, A., 2015. SIFT2: Enabling dense quantitative assessment of brain white matter connectivity using streamlines tractography. Neuroimage 119, 338–351. https://doi.org/10.1016/j.neuroimage.2015.06.092.

Yeo, B.T.T., Krienen, F.M., Sepulcre, J., Sabuncu, M.R., Lashkari, D., Hollinshead, M., et al., 2011. The organization of the human cerebral cortex estimated by intrinsic functional connectivity. J. Neurophysiol. 106, 1125–1165. https://doi.org/10.1152/jn.00338.2011.

Rubinov, M., Sporns, O., 2010. Complex network measures of brain connectivity: Uses and interpretations. Neuroimage 52, 1059–1069. https://doi.org/10.1016/j.neuroimage.2009.10.003.

Sporns, O., 2014. Contributions and challenges for network models in cognitive neuroscience. Nat. Neurosci. 17, 652–660. https://doi.org/10.1038/nn.3690.

Lohmann, G., Margulies, D.S., Horstmann, A., Pleger, B., Lepsien, J., Goldhahn, D., et al., 2010. Eigenvector Centrality Mapping for Analyzing Connectivity patterns in fMRI Data of the Human Brain. PLoS One 5, e10232. https://doi.org/10.1371/journal.pone.0010232.

Beynel, L., Powers, J.P., Appelbaum, L.G., 2020. Effects of repetitive transcranial magnetic stimulation on resting-state connectivity: a systematic review. Neuroimage 211, 116596. https://doi.org/10.1016/j.neuroimage.2020.116596.

Zhong, M., Cywiak, C., Metto, A.C., Liu, X., Qian, C., Pelled, G., 2021. Multi-session delivery of synchronous rTMS and sensory stimulation induces long-term plasticity. Brain Stimulation: Basic, Translational, and Clinical Research in Neuromodulation 14, 884–894. https://doi.org/10.1016/j.brs.2021.05.005.

Michael, N., Gösling, M., Reutemann, M., Kersting, A., Heindel, W., Arolt, V., et al., 2003. Metabolic changes after repetitive transcranial magnetic stimulation (rTMS) of the left prefrontal cortex: a sham-controlled proton magnetic resonance spectroscopy (1H MRS) study of healthy brain. Eur. J. Neurosci. 17, 2462–2468. https://doi.org/10.1046/j.1460-9568.2003.02683.x.

Karabanov, A., Ziemann, U., Hamada, M., George, M.S., Quartarone, A., Classen, J., et al., 2015. Consensus Paper: probing Homeostatic Plasticity of Human Cortex with Non-invasive Transcranial Brain Stimulation. Brain Stimul. 8, 993–1006. https://doi.org/10.1016/j.brs.2015.06.017.

Rosen, A.C., Bhat, J.V., Cardenas, V.A., Ehrlich, T.J., Horwege, A.M., Mathalon, D.H., et al., 2021. Targeting location relates to treatment response in active but not sham rTMS stimulation. Brain Stimul. 14, 703–709. https://doi.org/10.1016/j.brs.2021.04.010.

Momi, D., Ozdemir, R.A., Tadayon, E., Boucher, P., Di Domenico, A., Fasolo, M., et al., 2021. Perturbation of resting-state network nodes preferentially propagates to structurally rather than functionally connected regions. Sci. Rep. 11, 12458. https://doi.org/10.1038/s41598-021-90663-z.

Lai, Y., Dai, L., Wang, T., Zhang, Y., Zhao, Y., Wang, F., et al., 2023. Structural and functional correlates of the response to deep brain stimulation at ventral capsule/ventral striatum region for treatment-resistant depression. J. Neurol. Neurosurg. Psychiatry 94, 379–388. https://doi.org/10.1136/jnnp-2022-329702.

Mandke, K., Meier, J., Brookes, M.J., O'Dea, R.D., Van Mieghem, P., Stam, C.J., et al., 2018. Comparing multilayer brain networks between groups: introducing graph metrics and recommendations. Neuroimage 166, 371–384. https://doi.org/10.1016/j.neuroimage.2017.11.016.

Morriss, R., Briley, P.M., Webster, L., Abdelghani, M., Barber, S., Bates, P., et al., 2024. Connectivity-guided intermittent theta burst versus repetitive transcranial magnetic stimulation for treatment-resistant depression: a randomized controlled trial. Nat. Med. 30, 403–413. https://doi.org/10.1038/s41591-023-02764-z.

Tewarie, P., van Dellen, E., Hillebrand, A., Stam, C.J., 2015. The minimum spanning tree: an unbiased method for brain network analysis. Neuroimage 104, 177–188. https://doi.org/10.1016/j.neuroimage.2014.10.015.

Li, P., Yang, X., Greenshaw, A.J., Li, S., Luo, J., Han, H., et al., 2018. The effects of cognitive behavioral therapy on resting-state functional brain network in drug-naive patients with obsessive–compulsive disorder. Brain Behav. 8 (5), e00963. https://doi.org/10.1002/brb3.963.

Machado-Sousa, M., Bertolín, S., Picó-Pérez, M., Costa, A.D., Vieira, R., Alonso, P., et al., 2025. Neurobiological correlates of CBT response in OCD through the analysis of resting state networks. Int. J. Clin. Health Psychol. 25 (2), 100585. https://doi.org/10.1016/j.ijchp.2025.100585.

Yuan, S., Wu, H., Wu, Y., Xu, H., Yu, J., Zhong, Y., et al., 2022. Neural effects of cognitive behavioral therapy in psychiatric disorders: a systematic review and activation likelihood estimation meta-analysis. Front. Psychol. 13, 853804. https://doi.org/10.3389/fpsyg.2022.853804.

Rothman, K.J., 1990. No Adjustments are Needed for Multiple Comparisons. Epidemiology 1 (1), 43–46.

Streiner, D.L., Norman, G.R., 2011. Correction for Multiple Testing: is there a Resolution? Chest 140 (1), 16–18. https://doi.org/10.1378/chest.11-0523.

Feise RJ. Do multiple outcome measures require p-value adjustment? *BMC Med Res Methodol* 2002;2:8. https://doi.org/10.1186/1471-2288-2-8.

Uitenbroek DG. Bonferroni correction. SISA — Simple Interactive Statistical Analysis. 1997. Available at: http://www.quantitativeskills.com/sisa/calculations/bonfer.htm. Archived at: https://web.archive.org/web/20240725191050/http://www.quantitativeskills.com/sisa/calculations/bonfer.htm. Accessed July 25, 2024.